Synthesis, Structural Characterization, and Some Properties of New N-Functionally Substituted Diiron Azadithiolate Complexes as Biomimetic Models of Iron-Only Hydrogenases

Li-Cheng Song,* Bang-Shao Yin, Yu-Long Li, Li-Qun Zhao, Jian-Hua Ge, Zhi-Yong Yang, and Qing-Mei Hu

Department of Chemistry, State Key Laboratory of Elemento-Organic Chemistry, Nankai University, Tianjin 300071, People's Republic of China

Received May 30, 2007

The new N-functionally substituted azadithiolate ADT-type model complexes **2**−**9** have been synthesized starting from the known complex $[(\mu\text{-}SCH_2)_2NCH_2CH_2OH]Fe_2(CO)_6$ (**1**). Treatment of **1** with a halogenating agent, a mixture of PPh_3 and CBr_4, affords $[(\mu\text{-}SCH_2)_2NCH_2CH_2Br]Fe_2(CO)_6$ (**2**). Further treatment of **2** with MeC(O)SNa gives $[(\mu\text{-}SCH_2)_2NCH_2CH_2SC(O)Me]Fe_2(CO)_6$ (**3**). While **1** reacts with the acylating reagent 1-naphthaleneacetyl, 2-furancarbonyl, or 2-thiophenecarbonyl chloride to produce $[(\mu\text{-}SCH_2)_2NCH_2CH_2O_2CCH_2C_{10}H_7\text{-}1]Fe_2(CO)_6$ (**4**) and $[(\mu\text{-}SCH_2)_2NCH_2CH_2O_2CC_4H_3X\text{-}2]Fe_2(CO)_6$ (**6**, X = O; **7**, X = S), the CO substitution reaction of **4** with PPh_3 yields $[(\mu\text{-}SCH_2)_2NCH_2CH_2O_2CCH_2C_{10}H_7\text{-}1]Fe_2(CO)_5(PPh_3)$ (**5**). In the presence of the esterification catalyst 4-dimethylaminopyridine (DMAP) and the esterification activator *N*,*N*′-dicyclohexylcarbodiimide (DCC), **1** reacts with $CH_2(CO_2H)_2$ to give the unexpected single model complex $[(\mu\text{-}SCH_2)_2NCH_2CH_2O_2CMe]Fe_2(CO)_6$ (**8**), whereas reaction of **1** with *p*-$(HO_2C)_2C_6H_4$ under similar conditions affords the double model complex $[(\mu\text{-}SCH_2)_2NCH_2CH_2\text{-}Fe_2(CO)_6]_2[1,4\text{-}(O_2C)_2C_6H_4]$ (**9**). Starting complex **1** is found to be prepared in a much higher yield by another method, which involves reaction of $NH_2CH_2CH_2OH$ with the in situ formed intermediate $(\mu\text{-}HOCH_2S)_2Fe_2(CO)_6$ from CH_2O and $(\mu\text{-}HS)_2Fe_2(CO)_6$. The X-ray crystallographic study reveals that while the N-functional substituents of **1**, **3**, and **8** are axially bonded to their N atoms, the N-substituent of **7** is equatorially bound to its N atom. The IR spectra of **3** and **7** with CF_3SO_3H or CF_3CO_2H along with their ^1H NMR spectra with CF_3CO_2H or HOAc indicate that their bridgehead N atoms are protonated by strong acid CF_3SO_3H and partially protonated by the medium strong acid CF_3CO_2H, but not by weak acid HOAc. The electrochemical properties of **2**, **3**, **6**, and **7** are studied by CV and CA techniques, whereas **7** is further found to be a catalyst for H_2 production under electrochemical conditions. A 2E2C mechanism for this electrocatalytic H_2 evolution has been proposed, which is consistent with the above-mentioned protonation study of **7**.

Introduction

Research interest in the chemistry of butterfly dithiolate-bridged diiron complexes of the prototypal $(\mu\text{-}RS)_2Fe_2(CO)_6$ derivatives first reported by Reihlen in 1928[1] has been extensively revived in recent years,[2−5] due to the realization that they closely resemble the diiron subsite of Fe-only hydrogenases. X-ray crystallographic[6−9] and IR[10−12] studies have revealed that the active site of Fe-only hydrogenases (so-called H-cluster) comprises a diiron subsite that carries four unusual ligands: CO, CN^-, a cysteinyl-S-substituted cubic Fe_4S_4 cluster, and a three-light-atoms (possibly carbon or any combination of C, N, and O)-containing dithiolate ligand. This dithiolate was recently further suggested as an azadithiolate (ADT) SCH_2NCH_2S,[13] in which the bridgehead N atom plays an important role in the heterolytic cleavage or formation of hydrogen catalyzed by the natural enzymes (Scheme 1).[14]

* To whom correspondence should be addressed. Fax: 0086-22-23504853. E-mail: lcsong@nankai.edu.cn.

(1) Reihlen, H.; von Friedolsheim, A.; Oswald, W. *J. Liebigs Ann. Chem.* **1928**, *465*, 72.

(2) For reviews, see for example: (a) Darensbourg, M. Y.; Lyon E. J.; Smee, J. J. *Coord. Chem. Rev.* **2000**, *206*−*207*, 533. (b) Evans, D. J.; Pickett, C. J. *Chem. Soc. Rev.* **2003**, *32*, 268.

(3) For PDT diiron derivatives, see for example: (a) Gloaguen, F.; Lawrence, J. D.; Schmidt, M.; Wilson, S. R.; Rauchfuss, T. B. *J. Am. Chem. Soc.* **2001**, *123*, 12518. (b) Lyon, E. J.; Georgakaki, I. P.; Reibenspies, J. H.; Darensbourg, M. Y. *J. Am. Chem. Soc.* **2001**, *123*, 3268. (c) Razavet, M.; Davies, S. C.; Hughes, D. L.; Barclay, J. E.; Evans, D. J.; Fairhurst, S. A.; Liu, X.; Pickett, C. J. *Dalton Trans.* **2003**, 586. (d) Song, L.-C.; Cheng, J.; Yan, J.; Wang, H.-T.; Liu, X.-F.; Hu, Q.-M. *Organometallics* **2006**, *25*, 1544.

(4) For ADT diiron derivatives, see for example: (a) Lawrence, J. D.; Li. H.; Rauchfuss, T. B. *Chem. Commun.* **2001**, 1482. (b) Song, L.-C.; Ge, J.-H.; Zhang, X.-G.; Liu, Y.; Hu, Q.-M. *Eur. J. Inorg. Chem.* **2006**, 3204. (c) Schwartz, L.; Eilers, G.; Eriksson, L.; Gogoll, A.; Lomoth, R.; Ott, S. *Chem. Commun.* **2006**, 520.

(5) For ODT and TDT diiron derivatives, see for example: (a) Song, L.-C.; Yang, Z.-Y.; Bian, H.-Z.; Hu, Q.-M. *Organometallics* **2004**, *23*, 3082. (b) Song, L.-C.; Yang, Z.-Y.; Hua, Y.-J.; Wang, H.-T.; Liu, Y.; Hu, Q.-M. *Organometallics* **2007**, *26*, 2106.

(6) Peters, J. W.; Lanzilotta, W. N.; Lemon, B. J.; Seefeldt, L. C. *Science* **1998**, *282*, 1853.

(7) Nicolet, Y.; Piras, C.; Legrand, P.; Hatchikian, E. C.; Fontecilla-Camps, J. C. *Structure* **1999**, *7*, 13.

(8) Nicolet, Y.; De Lacey, A. L.; Vernède, X.; Fernandez, V. M.; Hatchikian, E. C.; Fontecilla-Camps, J. C. *J. Am. Chem. Soc.* **2001**, *123*, 1596.

(9) Lemon, B. J.; Peters, J. W. *Biochemistry* **1999**, *38*, 12969.

(10) Pierik, A. J.; Hulstein, M.; Hagen, W. R.; Albracht, S. P. J. *Eur. J. Biochem.* **1998**, *258*, 572.

(11) De Lacey, A. L.; Stadler, C.; Cavazza, C.; Hatchikian, E. C.; Fernandez, V. M. *J. Am. Chem. Soc.* **2000**, *122*, 11232.

(12) Chen, Z.; Lemon, B. J.; Huang, S.; Swartz, D. J.; Peters, J. W.; Bagley, K. A. *Biochemistry* **2002**, *41*, 2036.

10.1021/om7005326 CCC: $37.00
Publication on Web 08/29/2007

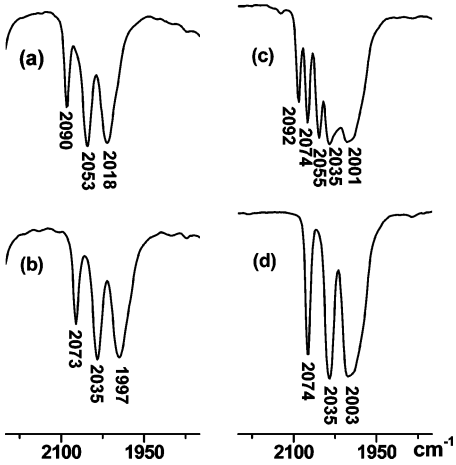

Figure 1. IR spectra of (a) **3** with CF_3SO_3H in MeCN, (b) neat **3** in MeCN, (c) **3** with CF_3CO_2H in $CHCl_3$, and (d) neat **3** in $CHCl_3$.

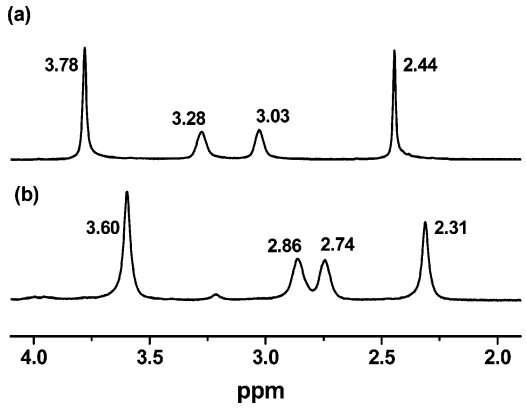

Figure 2. ^1H NMR spectra of (a) **3** with CF_3CO_2H and (b) neat **3**.

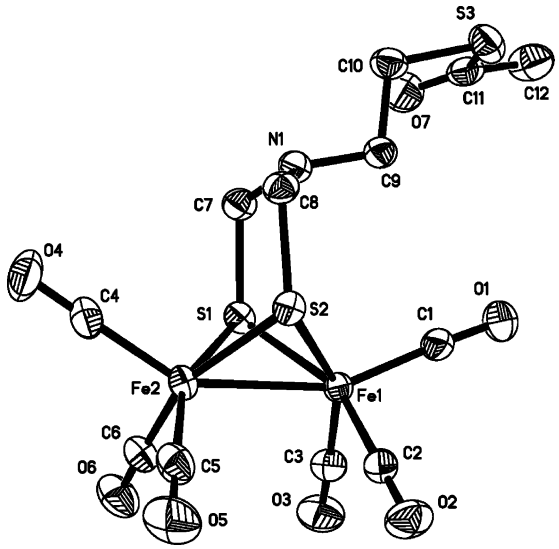

Figure 3. Molecular structure of **3** with 30% probability level ellipsoids.

In view of such biologically important functions played by the bridgehead N atom of the azadithiolate ligand in the H-cluster, chemists are interested in diiron ADT-type model complexes, particularly those complexes with organic functionalities at their azadithiolate N atoms. This is because such complexes can serve not only as simple models but also as starting materials to allow one to be able to attach a photosensitizer in order to obtain light-driven-type models[15,16] or to connect a cubic Fe_4S_4 cluster for making whole H-cluster skeleton models[17] through functional transformation reactions. In this paper, we report the synthesis, structural characterization, and electrochemical properties of a new series of N-functionally substituted diiron ADT-type models. In addition, the biomimetic H_2 evolution catalyzed by one of such models is also described.

Scheme 1

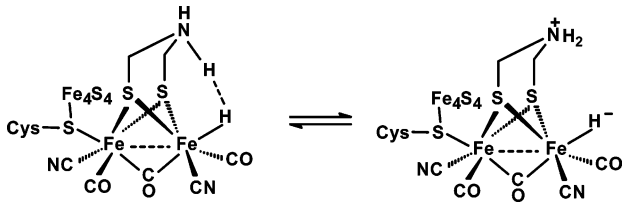

Results and Discussion

Synthesis and Characterization of $[(\mu\text{-}SCH_2)_2NCH_2CH_2OH]Fe_2(CO)_6$ (1), $[(\mu\text{-}SCH_2)_2NCH_2CH_2Br]Fe_2(CO)_6$ (2), and $[(\mu\text{-}SCH_2)_2NCH_2CH_2SC(O)Me]Fe_2(CO)_6$ (3). We prepared the N-hydroxyethyl-substituted model complex **1** in 80% yield by a sequential reaction of the in situ prepared $(\mu\text{-}HS)_2Fe_2(CO)_6$[18] with 2 equiv of 37% aqueous formaldehyde, followed by treatment of the intermediate $(\mu\text{-}HOCH_2S)_2Fe_2(CO)_6$ with 1 equiv of $NH_2CH_2CH_2OH$, according to the Rauchfuss method[19] (Scheme 2).

Although **1** was previously prepared by others[20] using a similar method,[21] the yield is very low (only 25%) and a large (10-fold) excess of the starting materials $NH_2CH_2CH_2OH$ and paraformaldehyde (relative to $(\mu\text{-}HS)_2Fe_2(CO)_6$) was used. The characterizing data for our **1** are basically the same as those for the previously reported one, except that our **1** displayed a broad singlet centered at 1.66 ppm for its OH group, which completely disappeared in the presence of D_2O due to D/H exchange. Our complex **1** was confirmed by X-ray diffraction analysis (see the Supporting Information), which is essentially the same as that previously reported.[20] Indeed, it contains a butterfly Fe_2S_2 cluster core that is bridged by a N-hydroxyethyl-substituted azapropylene group to form two fused six-membered FeSCNCS rings with a chair and a boat conformations, respectively. The Fe−Fe bond length of 2.5015 Å for **1** is somewhat shorter than those (2.55−2.62 Å) in the oxidized and reduced forms of Fe-only hydrogenases[6−8] and is in agreement with the Fe−Fe bond lengths found for other diiron dithiolate model complexes.[3c,4a,22−24]

(13) (a) Nicolet, Y.; Lemon, B. J.; Fontecilla-Camps, J. C.; Peters, J. W. *Trends Biochem. Sci.* **2000**, *25*, 138. (b) Nicolet, Y.; Lacey, A. L.; Vernede, X.; Fernandez, V. M.; Hatchikian, E. C.; Fontecilla-Camps, J. C. *J. Am. Chem. Soc.* **2001**, *123*, 1596.

(14) Fan, H.; Hall, M. B. *J. Am. Chem. Soc.* **2001**, *123*, 3828.

(15) Song, L.-C.; Tang, M.-Y.; Su, F.-H.; Hu, Q.-M. *Angew. Chem., Int. Ed.* **2006**, *45*, 1130.

(16) Song, L.-C.; Tang, M.-Y.; Mei, S.-Z.; Huang, J.-H.; Hu, Q.-M. *Organometallics* **2007**, *26*, 1575.

(17) Tard, C.; Liu, X.; Ibrahim, S. K.; Bruschi, M.; De Giola, L.; Davies, S. C.; Yang, X.; Wang, L.-S.; Sawers, G.; Pickett, C. J. *Nature* **2005**, *433*, 610.

(18) Seyferth, D.; Henderson, R. S.; Song, L.-C. *J. Organomet. Chem.* **1980**, *192*, C1.

(19) Stanley, J. L.; Rauchfuss, T. B.; Wilson, S. R. *Organometallics* **2007**, *26*, 1907.

(20) Cui, H.-G.; Wang, M.; Dong, W.-B.; Duan, L.-L.; Li, P.; Sun, L. *Polyhedron* **2007**, *26*, 904.

(21) Li, H; Rauchfuss, T. B. *J. Am. Chem. Soc.* **2002**, *124*, 726.

(22) Lyon, E. J.; Georgakaki, I. P.; Reibenspies, J. H.; Darensbourg, M. Y. *Angew. Chem., Int. Ed.* **1999**, *38*, 3178.

(23) Lawrence, J. D.; Li, H.; Rauchfuss, T. B.; Bénard, M.; Rohmer, M.-M. *Angew. Chem., Int. Ed.* **2001**, *40*, 1768.

(24) Song, L.-C.; Ge, J.-H.; Liu, X.-F.; Zhao, L.-Q.; Hu, Q.-M. *J. Organomet. Chem.* **2006**, *691*, 5701.

Scheme 2

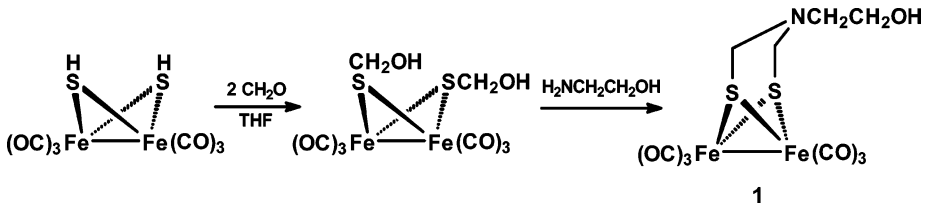

Scheme 3

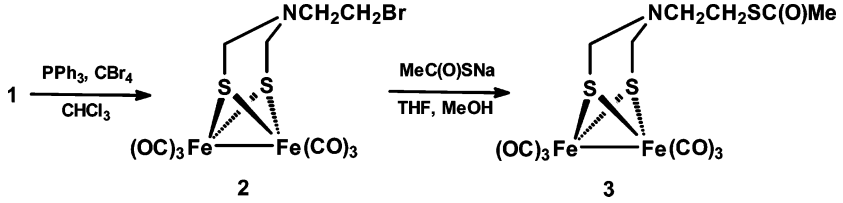

Table 1. Selected Bond Lengths (Å) and Angles (deg) for 3, 7, and 8

		3	
Fe(1)−S(1)	2.2769(8)	Fe(2)−S(2)	2.2659(8)
Fe(1)−S(2)	2.2664(8)	S(3)−C(10)	1.808(3)
Fe(1)−Fe(2)	2.5027(5)	C(11)−O(7)	1.199(4)
Fe(2)−S(1)	2.2628(8)	N(1)−C(7)	1.427(3)
S(2)−Fe(1)−S(1)	84.04(3)	S(2)−Fe(1)−Fe(2)	56.47(2)
S(1)−Fe(2)−Fe(1)	56.81(2)	S(1)−Fe(1)−Fe(2)	56.28(2)
S(2)−Fe(2)−Fe(1)	56.49(2)	S(1)−Fe(2)−S(2)	84.37(3)
Fe(2)−S(1)−Fe(1)	66.91(2)	O(7)−C(11)−C(12)	123.9(4)
Fe(2)−S(2)−Fe(1)	67.03(2)	C(7)−N(1)−C(8)	115.1(2)
		7	
Fe(1)−S(1)	2.2525(11)	Fe(2)−S(2)	2.2485(12)
Fe(1)−S(2)	2.2513(11)	N(1)−C(7)	1.437(5)
Fe(1)−Fe(2)	2.5096(8)	C(11)−O(7)	1.334(5)
Fe(2)−S(1)	2.2507(12)	C(11)−O(8)	1.210(5)
S(2)−Fe(1)−S(1)	85.30(4)	S(2)−Fe(1)−Fe(2)	56.05(3)
S(1)−Fe(2)−Fe(1)	56.16(3)	S(1)−Fe(1)−Fe(2)	56.10(3)
S(2)−Fe(2)−Fe(1)	56.15(3)	S(2)−Fe(2)−S(1)	85.41(4)
Fe(2)−S(1)−Fe(1)	67.74(4)	O(8)−C(11)−O(7)	123.8(4)
Fe(2)−S(2)−Fe(1)	67.80(3)	C(8)−N(1)−C(7)	114.0(3)
		8	
Fe(1)−S(1)	2.2628(6	Fe(2)−S(2)	2.2637(6)
Fe(1)−S(2)	2.2561(6)	O(7)−C(11)	1.347(2)
Fe(1)−Fe(2)	2.5114(5)	O(8)−C(11)	1.200(2)
Fe(2)−S(1)	2.2569(6)	N(1)−C(7)	1.418(2)
S(2)−Fe(1)−S(1)	84.74(2)	S(2)−Fe(2)−Fe(1)	56.103(17)
S(2)−Fe(1)−Fe(2)	56.388(16)	Fe(2)−S(1)−Fe(1)	67.512(18)
S(1)−Fe(1)−Fe(2)	56.131(17)	Fe(1)−S(2)−Fe(2)	67.509(18)
S(1)−Fe(2)−S(2)	84.70(2)	O(8)−C(11)−C(12)	125.40(19)
S(1)−Fe(2)−Fe(1)	56.356(16)	C(7)−N(1)−C(8)	116.23(15)

Scheme 4

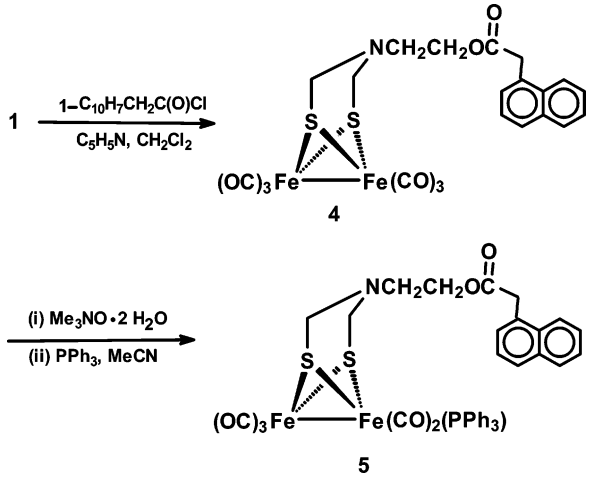

Scheme 5

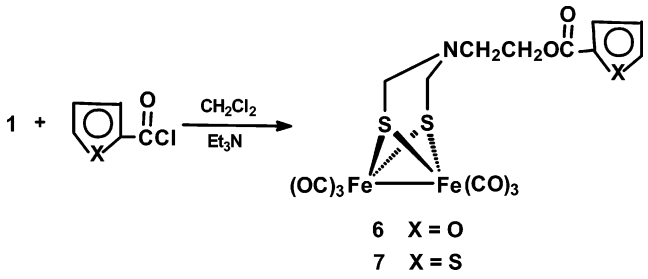

On the basis of the improved synthesis and full characterization of model complex **1**, we prepared some new N-functionally substituted ADT-type models by its functional transformation reactions. For instance, treatment of **1** with a halogenating reagent, a mixture of PPh_3 and CBr_4,[25] in $CHCl_3$ at room temperature resulted in formation of the *N*-bromoethyl model complex **2** in 59% yield; further treatment of **2** with 1 equiv of MeC(O)SNa in THF/MeOH at room temperature gave rise to the *N*-acetylthioethyl model complex **3** in 60% yield (Scheme 3).

Complexes **2** and **3** were characterized by elemental analysis and IR and ^{1}H NMR spectroscopy. For example, the IR spectra of **2** in KBr disk and **3** in KBr disk, in MeCN or in $CHCl_3$, displayed three to four absorption bands in the range 2074−1971 cm^{-1} for their terminal carbonyls. In addition, the ^{1}H NMR spectra of **2** and **3** in $CDCl_3$ exhibited a singlet around 3.7 ppm for the two identical protons in each of their two NCH_2S groups. Interestingly, in the IR spectrum of **3** with CF_3SO_3H in MeCN, the three $\nu_{C\equiv O}$ bands at 2090, 2053, and 2018 cm^{-1} are shifted 17−21 cm^{-1} to higher energy relative to that without CF_3SO_3H (Figure 1). This implies that the bridgehead N atom of **3**, similar to that of $[(\mu\text{-}SCH_2)_2NMe]Fe_2(CO)_6$ reported by Rauchfuss,[23] is completely protonated by the strong acid CF_3SO_3H (pK_a = 1.57 in MeCN). However, in contrast to this, the bridgehead N atom of **3** can only be partially protonated by the medium strong acid CF_3CO_2H (pK_a = 12.65 in MeCN), as its IR spectrum in $CHCl_3$ showed five absorption bands at 2092, 2074, 2055, 2035, and 2001 cm^{-1}, which is actually the total spectrum displayed by free and protonated **3** (Figure 1). The ^{1}H NMR signals of **3** in $CDCl_3$ with CF_3CO_2H are shifted toward low field by 0.13−0.42 ppm relative to those of **3** without CF_3CO_2H (Figure 2), but those of **3** with HOAc are basically the same as those of **3**

(25) Verheyden, J. P. H.; Moffatt, J. G. *J. Org. Chem.* **1972**, *37*, 2289.

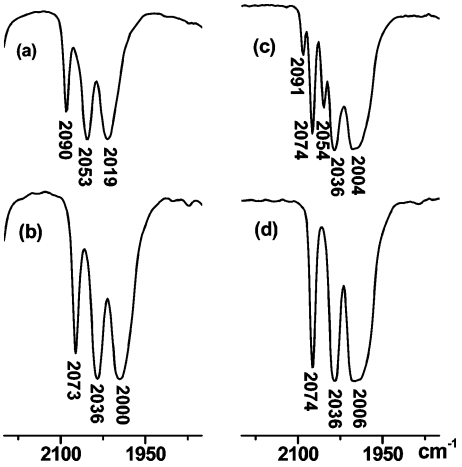

Figure 4. IR spectra of (a) **7** with CF_3SO_3H in MeCN, (b) neat **7** in MeCN, (c) **7** with CF_3CO_2H in $CHCl_3$, and (d) neat **7** in $CHCl_3$.

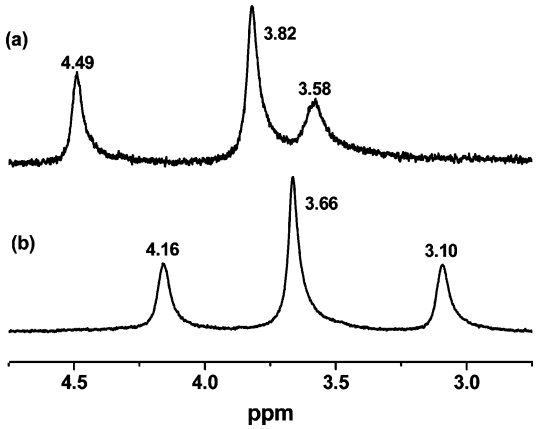

Figure 5. Partial ^1H NMR spectra of (a) **7** with CF_3CO_2H and (b) neat **7**.

itself. Such ^1H NMR observations are consistent with the fact that the bridgehead N atom of **3** can be protonated by the medium strong acid CF_3CO_2H but not by weak acid HOAc (pK_a = 22.6 in MeCN). However, in contrast to the corresponding IR spectrum, no signals of free **3** were observed in the ^1H NMR spectrum of **3** with CF_3CO_2H, which is probably due to the too fast interconversion between free **3** and the partially protonated **3** during the ^1H NMR determination.

The crystallographic study of **3** (Figure 3, Table 1) revealed that the C11−O7 double bond (1.199 Å) in its acetylthio group is much shorter than the single bond C10−O7 in the hydroxylethyl group of **1** (1.378 Å; see the Supporting Information), which is consistent with its IR spectrum displaying a strong band at 1670 cm^{-1}. The Fe−Fe bond length (2.5027 Å) of **3** is almost the same as that (2.5015 Å) of **1**. In addition, both the *N*-acetylthioethyl functionality of **3** and the hydroxyethyl functionality of **1** are axially bonded to the bridgehead N atoms of their azadithiolate ligands.

Synthesis and Characterization of [(μ-SCH_2)$_2$$NCH_2CH_2O_2$-$CCH_2C_{10}H_7$-1]$Fe_2(CO)_5L$ (4, L = CO; 5, L = PPh_3) and [(μ-SCH_2)$_2$$NCH_2CH_2O_2CC_4H_3$X-2]$Fe_2(CO)_6$ (6, X = O; 7, X = S). Further functional transformation reaction of **1** with excess 1-naphthylacetyl chloride in CH_2Cl_2 from 0 °C to room temperature in the presence of pyridine afforded its naphthylacetic ester model complex **4** in 77% yield; subsequent CO substitution of **4** with 1 equiv of decarbonylating agent $Me_3NO{\cdot}2H_2O$[3a] in MeCN at room temperature, followed by 1 equiv of PPh_3 (phosphines are good surrogates for the cyanide ligand found in the enzyme[26,27]), produced the mono-Ph_3P-substituted model complex **5** in 83% yield (Scheme 4).

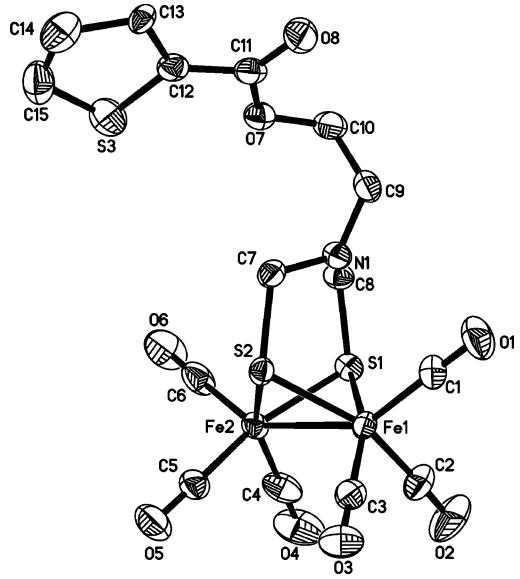

Figure 6. Molecular structure of **7** with 30% probability level ellipsoids.

While complex **4** is a red oil, **5** is a red solid, both easily soluble in common solvents such as CH_2Cl_2 and acetone. Complexes **4** and **5** were also characterized by elemental analysis and spectroscopy. The IR spectra of **4** and **5** displayed three absorption bands in the range 2072−1929 cm^{-1} for their terminal carbonyls, but it is noteworthy that the absorption bands of **5** lie at much lower frequencies than those of **4** (lowering 28−43 cm^{-1}), obviously due to the increased back-bonding in **5** caused by CO substitution of **4** with the stronger electron-donating PPh_3.[28] The ^1H NMR spectrum of **4** displayed a singlet at 3.06 ppm for the two identical protons in each of its two NCH_2S groups, whereas **5** exhibited two doublets at 2.27 and 2.65 ppm for the two different protons in each of its two NCH_2S groups. In fact, the two protons in each of their two NCH_2S groups of **4** and **5** are all diastereotopic and thus magnetically different. However, for **4** the interconversion between the two fused six-membered rings FeSCNCS in its diiron ADT moiety is too fast to distinguish the two diastereotopic protons by ^1H NMR determination at room temperature.[23] The ^{31}P NMR spectrum of **5** showed a singlet at 66.02 ppm, which is very close to those displayed by the PPh_3-coordinated diiron complexes.[27]

Similar to the preparation of model complex **4**, when **1** reacted with excess 2-furancarbonyl or 2-thiophenecarbonyl chloride in CH_2Cl_2 in the presence of Et_3N at room temperature, the corresponding ester model complexes **6** and **7** were obtained in 80% and 62% yields, respectively (Scheme 5).

Complexes **6** and **7** are air-stable, red solids, which have been fully characterized by elemental analysis and IR and ^1H NMR spectroscopy. For instance, the IR spectra of **6** in KBr disk and **7** in KBr disk, in MeCN or in $CHCl_3$, displayed three to four absorption bands in the region 2074−1973 cm^{-1} for their terminal carbonyls. In addition, they showed a singlet at ca.

(26) Zhao, X.; Chiang, C.-Y.; Miller, M. L.; Rampersad, M. V.; Darensbourg, M. Y. *J. Am. Chem. Soc.* **2003**, *125*, 518.

(27) Song, L.-C.; Yang, Z.-Y.; Bian, H.-Z.; Liu, Y.; Wang, H.-T.; Liu, X.-F.; Hu, Q.-M. *Organometallics* **2005**, *24*, 6126.

(28) Collman, J. P.; Hegedus, L. S. *Principles and Applications of Organotransition Metal Chemistry*; University Science Books: Mill Valley, CA, 1980.

Scheme 6

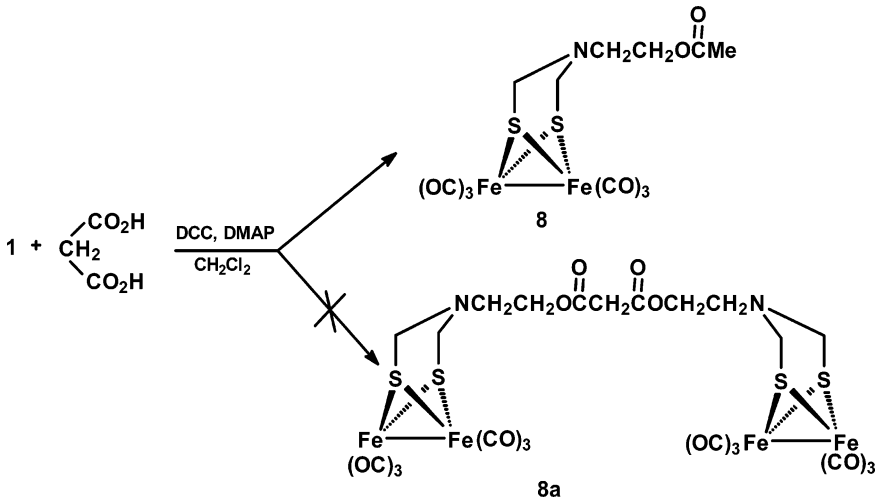

Scheme 7

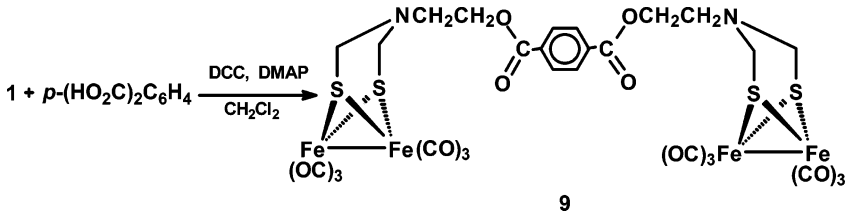

3.6 ppm for the two identical protons in each of their two NCH_2S groups. Similar to **3**, the basic bridgehead N atom can be also completely protonated by the strong acid CF_3SO_3H and partially protonated by the medium strong acid CF_3CO_2H, but not by weak acid HOAc. These have been proved by the following spectroscopic observations: (i) the IR spectrum of **7** with CF_3SO_3H exhibited three bands at 2090, 2053, and 2019 cm^{-1}, which are shifted 17−19 cm^{-1} to higher energy compared to that without CF_3SO_3H (Figure 4); (ii) the IR spectrum of **7** with CF_3CO_2H displayed five bands at 2091, 2074, 2054, 2036, and 2004 cm^{-1} for the terminal carbonyls of free and protonated **7** (Figure 4); and (iii) the ^1H NMR signals of the groups NCH_2S and NCH_2CH_2O of **7** with CF_3CO_2H are downfield shifted by 0.16−0.48 ppm relative to those of **7** without CF_3CO_2H (Figure 5).

The molecular structure of **7** was unambiguously confirmed by crystallographic study (Figure 6, Table 1). This structure has an *N*-thiophenecarboxyethyl functionality, in which the C11−O8 double bond length is 1.210 Å. The dihedral angle between the thiophene ring and the O8−C11−O7 plane is only 0.9°. This implies that p−π conjugation exists between the thiophene ring and the O8−C11−O7 moiety. In addition, in contrast to **1** and **3**, the N-substituted functionality of **7** is attached to N1 by an equatorial bond of the two fused six-membered rings.

Synthesis and Characterization of [(μ-SCH_2)$_2$$NCH_2CH_2O_2CMe$]-$Fe_2(CO)_6$ (8) and [(μ-SCH_2)$_2$$NCH_2CH_2Fe_2(CO)_6$][1,4-$(O_2C)_2$-$C_6H_4$] (9). Double active-site models are of interest,[27,29] since they could provide the possibility to explore whether the catalysis occurs at the two active sites separately or synergistically. In order to prepare the double active-site models, we initially carried out the reaction of complex **1** with 0.5 equiv of malonic acid in the presence of the esterification catalyst 4-dimethylaminopyridine (DMAP) and the esterification activator *N*,*N*′-dicyclohexylcarbodiimide (DCC)[30] in CH_2Cl_2 from 0 °C to room temperature. As a result, the expected double model **8a** was not isolated, but instead, the single model **8** was obtained in 65% yield (Scheme 6).

Apparently, single model **8** is most likely generated by esterification of the *N*-hydroxyethyl complex **1** with acetic acid formed in situ by decarboxylation of malonic acid under such conditions. This is because (i) vigorous CO_2 evolution was observed during the reaction course; (ii) from the above-mentioned reaction mixture, about half of starting material **1** was recovered; and (iii) when the reaction of **1** with 1 equiv of malonic acid was carried out under similar conditions, **8** was obtained in 67% yield.

Interestingly, it was found that the aromatic dibasic acid *p*-phthalic acid, in contrast to malonic acid, reacted with 2 equiv of **1** under similar conditions gave the expected double active-site model **9** in 44% yield (Scheme 7).

The single and double active-site models **8** and **9** are air-stable, red solids, which were characterized by elemental analysis and spectroscopy. In the IR spectra they showed four absorption bands in the range 2068−1965 cm^{-1} for their terminal carbonyls and one absorption band at 1742 or 1711 cm^{-1} for their ester carbonyls. In the ^1H NMR spectra they displayed a singlet at ca. 3.60 ppm for their NCH_2S groups. The molecular structure of **8** was unequivocally confirmed by X-ray crystallography (Figure 7, Table 1). Indeed, it is a single active-site model in which an acetate group is bound to C10 of the *N*-acetoxyethyl functionality. In this molecule the C11−O8 double bond length (1.200 Å) in **8** is almost identical with those of C11−O7 (1.199 Å) in **3** and C11−O8 (1.210 Å) in **7**. In addition, the Fe−Fe bond length (2.5114 Å) of **8** is also nearly identical with those of **1** (2.5015 Å), **3** (2.5027 Å), and **7** (2.5096

(29) Kovacs, J. A.; Bashkin, J. K.; Holm, R. H. *J. Am. Chem. Soc.* **1985**, *107*, 1784.

(30) Neises, B.; Steglich, W. *Angew. Chem., Int. Ed. Engl.* **1978**, *17*, 522.

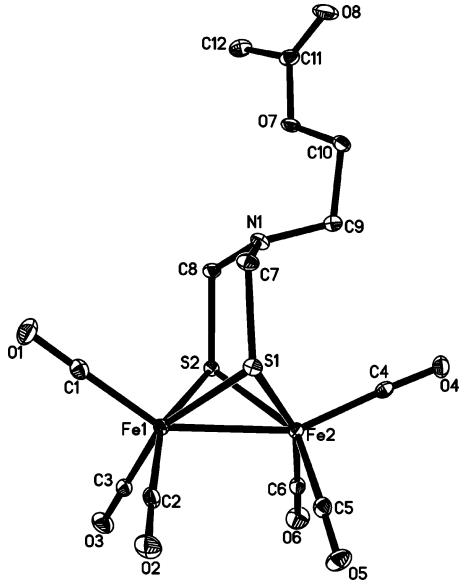

Figure 7. Molecular structure of **8** with 30% probability level ellipsoids.

Table 2. Electrochemical Data of 2, 3, 6, and 7

compound	E_{pc1} [V]	E_{pc2} [V]	E_{pa} [V]
2	−1.63	−2.33	+0.59
3	−1.62	−2.29	+0.56
6	−1.63	−2.10	+0.53
7	−1.64	−2.09	+0.56

Å). In fact, the structure is very similar to the above-described structures of **1**, **3**, and **7**, as well as the other azadithiolate-bridged diiron complexes.[4a,b,23]

Electrochemistry of 2, 3, 6, and 7. The electrochemical properties of **2**, **3**, **6**, and **7** were investigated by cyclic voltammetry (CV) in MeCN under CO atmosphere. While Table 2 lists their electrochemical data, Figures 8 and 9 show the cyclic voltammograms of **3** and **7**, respectively. It is shown that **2**, **3**, **6**, and **7** each display one quasi-reversible reduction process, one irreversible reduction process, and one irreversible oxidation process. All the first quasi-reversible reductions (E_{pc} = −1.62 to −1.64 V) are one-electron processes, which is supported by the calculated value of 0.9 faraday/equiv (obtained through study of bulk electrolysis of **7**) and the calculated value of $(i_p/v^{1/2})/(it^{1/2}) = 4.08$ (obtained through study of CV and chronoamperometry (CA) of **7**).[31] These one-electron processes can be assigned to the reduction of Fe^IFe^I to Fe^IFe^0. The second reductions (E_{pc} = −2.09 to −2.33 V) and the oxidations (E_{pa} = +0.53 to +0.59 V) are also one-electron processes, which can be ascribed to the reduction of Fe^IFe^0 to Fe^0Fe^0 and the oxidation of Fe^IFe^I to Fe^IFe^{II}, respectively. Interestingly, model **7** as a representative has been found to have the catalytic ability for proton reduction to hydrogen in the presence of acetic acid (HOAc) under CV conditions. As shown in Figure 10, upon addition of the first 2 mM HOAc to the solution of **7**, the initial first reduction peak at −1.64 V slightly increased but did not continue to grow up with sequential addition of the acid. However, in contrast to this, the initial second reduction peak at −2.09 V increased markedly and continued to increase with increasing concentration of the acid. These observations are consistent with an electrocatalytic proton reduction.[32−36] It is worth pointing out that acetic acid without **7** is reduced at a potential of −2.6 V; thus the reduction potential of HOAc with catalyst **7** is shifted positively by 300 mV. The electrocatalytic process was further confirmed by bulk electrolysis of a MeCN solution of **7** (0.50 mM) with HOAc (30 mM) at −2.30 V. During half an hour a total of 13.5 F per mol of **7** passed, which corresponds to 6.7 turnovers. GC analysis indicated that the hydrogen yield is about 90%.

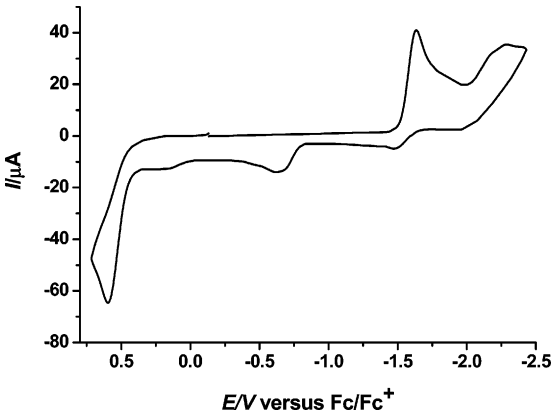

Figure 8. Cyclic voltammogram of **3** (1.0 mM) in 0.1 M *n*-Bu_4NPF_6/MeCN at a scan rate of 100 mV s^{-1}.

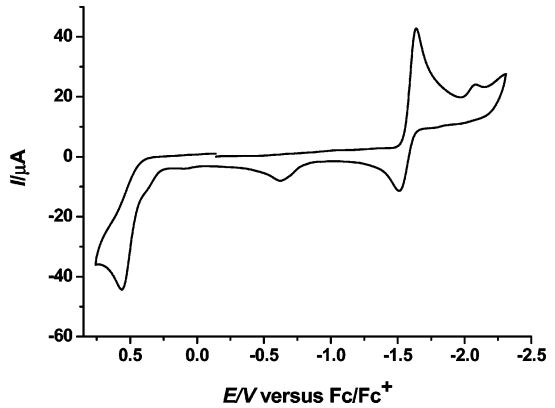

Figure 9. Cyclic voltammogram of **7** (1.0 mM) in 0.1 M *n*-Bu_4NPF_6/MeCN at a scan rate of 100 mV s^{-1}.

On the basis of similar cases[4b,27,35,36] and the above-mentioned electrochemical observations, a 2E2C (E = electrochemical, C = chemical) mechanism can be suggested to account for this electrocatalytic H_2 production. First, **7** (denoted as $[Fe^IFe^I]$) is reduced at −1.64 V to give monoanion $\mathbf{7}^-$. Then $\mathbf{7}^-$ is further reduced at −2.09 V to produce dianion $\mathbf{7}^{2-}$. After the electron-rich $\mathbf{7}^{2-}$ is protonated by HOAc to generate the Fe−H species $\mathbf{7H}^-$, it accepts an additional proton from HOAc to complete the catalytic cycle with H_2 evolution (Scheme 8). It should be noted that this mechanism is consistent with the above-mentioned ^{1}H NMR data of **7** with HOAc. That is, the catalytic cycle cannot start with the first protonation of **7** since it does not have a strong enough basic site (either the diiron center or the bridgehead N atom) to capture the weak acid HOAc protons.

(31) (a) Winter, R. F.; Geiger, W. G. *Organometallics* **2003**, *22*, 1948. (b) Zanello, P. *Inorganic Electrochemistry. Theory, Practice and Application*; Thomas Graham House: Cambridge, UK, 2003.

(32) Gloaguen, F.; Lawrence, J. D.; Rauchfuss, T. B. *J. Am. Chem. Soc.* **2001**, *123*, 9476.

(33) Chong, D.; Georgakaki, I. P.; Mejia-Rodriguez, R.; Sanabria-Chinchilla, J.; Soriaga, M. P.; Darensbourg, M. Y. *Dalton Trans.* **2003**, 4158.

(34) Bhugun, I.; Lexa, D.; Saveant, J.-M. *J. Am. Chem. Soc.* **1996**, *118*, 3982.

(35) Mejia-Rodriguez, R.; Chong, D.; Reibenspies, J. H.; Soriaga, M. P.; Darensbourg, M. Y. *J. Am. Chem. Soc.* **2004**, *126*, 12004.

(36) Capon, J.-F.; Gloaguen, F.; Schollhammer, P.; Talarmin, J. *Coord. Chem. Rev.* **2005**, *249*, 1664.

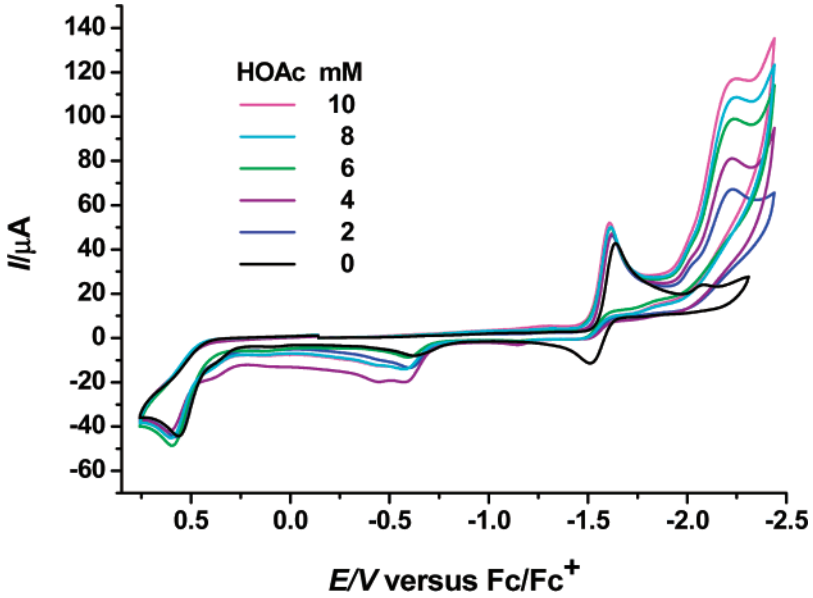

Figure 10. Cyclic voltammogram of **7** (1.0 mM) with HOAc (0−10 mM) in 0.1 M *n*-Bu_4NPF_6/MeCN at a scan rate of 100 mV s^{-1}.

Scheme 8

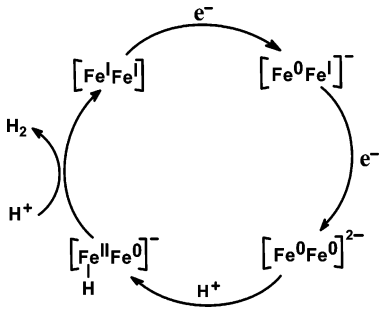

Thus, this mechanism is considerably different from the 2C2E mechanism suggested for the H_2 production from strong acid HOTs catalyzed by the PDT-type model, $[Fe_2(\mu\text{-PDT})_2(CO)_4(CN)(Me_3P)]^-$, in which the remarkably increased electron density at the Fe−Fe bond by substitution of the strongly donating Me_3P and CN^- ligands permits the first protonation in its catalytic cycle.[32]

Conclusion

On the basis of the improved synthesis of starting complex **1**, the new N-functionally substituted azadithiolate H-cluster models **2**−**9** have been synthesized through the functional transformation reactions of the *N*-hydroxyethyl functionality of **1** and the *N*-bromoethyl functionality of **2**, as well as the CO substitution reaction of **4**. Particularly noteworthy is that while double model complex **9** is synthesized from **1** and *p*-phthalic acid in the presence of DCC and DMAP, the single model complex **8** is produced unexpectedly from **1** and malonic acid under similar conditions due to decarboxylation of malonic acid. Complexes **1**−**9** have been characterized by elemental analysis and spectroscopy, and particularly for **1**, **3**, **7**, and **8** by X-ray crystallography. As a representative model, **7** has been proved to be a catalyst for proton reduction to hydrogen under CV conditions. In addition, a 2E2C mechanism for this catalytic reaction is suggested. Further study on attachment of such N-functionally substituted simple models to some photosensitizers to make new light-driven-type models is in progress in this laboratory.

Experimental Section

General Comments. All reactions were performed using standard Schlenk and vacuum-line techniques under N_2 atmosphere. Dichloromethane and chloroform were distilled over CaH_2 under N_2. Acetonitrile was distilled once from P_2O_5 and then from CaH_2 under N_2. THF was purified by distillation under N_2 from sodium/benzophenone ketyl. *N*,*N*′-Dicyclohexylcarbodiimide (DCC), 4-dimethylaminopyridine (DMAP), Et_3BHLi (1 M in THF), and other materials were available commercially and used as received. $(\mu\text{-S})_2Fe_2(CO)_6$,[37] 1-naphthylacetyl chloride [1-$C_{10}H_7CH_2C(O)Cl$],[38] furancarbonyl chloride [2-$C_4H_3OC(O)Cl$],[39] and thiophenecarbonyl chloride [2-$C_4H_3SC(O)Cl$][40] were prepared according to literature procedures. Preparative TLC was carried out on glass plates (26 × 20 × 0.25 cm) coated with silica gel H (10−40 μm). IR spectra were recorded on a Bruker Vector 22 or Bruker FT-IR Equinox 55 infrared spectrophotometer. ^1H (^{31}P) NMR spectra were obtained on a Bruker Avance 300 NMR or a Varian Mercury Plus 400 MHz NMR spectrometer. Elemental analyses were performed on an Elementar Vario EL analyzer. Melting points were determined on a Yanaco MP-500 apparatus and are uncorrected.

Preparation of $[(\mu\text{-SCH}_2)_2NCH_2CH_2OH]Fe_2(CO)_6$ (1). A red solution of $(\mu\text{-S})_2Fe_2(CO)_6$ (0.344 g, 1.0 mmol) in THF (15 mL) was cooled to −78 °C and then treated dropwise with Et_3BHLi (2 mL, 2.0 mmol) to give a green solution. After stirring for 15 min, CF_3CO_2H(0.16 mL, 2.0 mmol) was added to cause an immediate color change from green to red. The mixture was stirred for 10 min, and then 37% aqueous formaldehyde (0.17 mL, 2.0 mmol) was added. The new mixture was allowed to warm to room temperature and stirred at this temperature for 1 h. After $H_2NCH_2CH_2OH$ (0.07 mL, 1.1 mmol) was added, the new mixture was stirred for an additional 1 h. Volatiles were removed under vacuum, and the residue was subjected to TLC using CH_2Cl_2/petroleum ether (v/v = 2:1) as eluent. From the main red band, **1** was obtained as a red solid (0.344 g, 80%), mp 94−96 °C. Anal. Calcd for $C_{10}H_9Fe_2NO_7S_2$: C, 27.87; H, 2.10; N, 3.25. Found: C, 27.71; H, 2.25; N, 3.38. IR (KBr disk): $\nu_{C\equiv O}$ 2072 (s), 2035 (vs), 1997 (vs); ν_{O-H}

(37) Seyferth, D.; Henderson, R. S.; Song, L.-C. *Organometallics* **1982**, *1*, 125.
(38) Conry, R. R.; Striejewske, W. S.; Tipton, A. A. *Inorg. Chem.* **1999**, *38*, 2833.
(39) Chadwick, D. J.; McKnight, M. V.; Ngochindo, R. *J. Chem. Soc., Perkin Trans. 1* **1982**, 1343.
(40) Carpenter, A. J.; Chadwick, D. J. *J. Chem. Soc., Perkin Trans. 1* **1985**, 173.

3496 (m) cm^{-1}. ^1H NMR (300 MHz, $CDCl_3$): 1.66 (br s, 1H, OH), 2.86 (t, 2H, NCH_2CH_2O), 3.52 (d, 2H, NCH_2CH_2O), 3.60 (s, 4H, 2 NCH_2S) ppm.

Preparation of [(μ-SCH_2)$_2$$NCH_2CH_2Br$]$Fe_2(CO)_6$ (2). A red solution of **1** (0.862 g, 2.0 mmol), PPh_3 (1.310 g, 5.0 mmol), and CBr_4 (3.320 g, 10.0 mmol) in $CHCl_3$ (15 mL) was stirred at room temperature for 1 h until TLC showed that **1** was completely consumed. After volatiles were removed at reduced pressure, the residue was subjected to TLC using CH_2Cl_2/petroleum ether (v/v = 1:2) as eluent. From the main red band, **2** was obtained as a red solid (0.587 g, 59%), mp 87−89 °C. Anal. Calcd for $C_{10}H_8Fe_2NO_6S_2Br$: C, 24.32; H, 1.63; N, 2.84. Found: C, 24.45; H, 1.86; N, 2.81. IR (KBr disk): $\nu_{C\equiv O}$ 2070 (vs), 2030 (vs), 2010 (vs), 1990 (vs), 1971 (vs) cm^{-1}. ^1H NMR (400 MHz, $CDCl_3$): 3.18 (s, 4H, NCH_2CH_2Br), 3.72 (s, 4H, 2NCH_2S) ppm.

Preparation of [(μ-SCH_2)$_2$$NCH_2CH_2SC(O)Me$]$Fe_2(CO)_6$ (3). A solution of **2** (0.125 g, 0.25 mmol) and MeC(O)SNa (0.026 g, 0.26 mmol) in THF (15 mL) and MeOH (5 mL) was stirred at room temperature for 5 h until **2** was completely consumed. The same workup as that for the preparation of **2** gave **3** as a red solid (0.073 g, 60%), mp 92−93 °C. Anal. Calcd for $C_{12}H_{11}Fe_2NO_7S_3$: C, 29.47; H, 2.27; N, 2.86. Found: C, 29.30; H, 2.31; N, 3.02. IR (KBr disk): $\nu_{C\equiv O}$ 2071 (s), 2038 (vs), 2006 (vs), 1980 (s); $\nu_{C=O}$ 1690 (s) cm^{-1}. IR ($CHCl_3$): $\nu_{C\equiv O}$ 2074 (s), 2035 (vs), 2003 (vs); $\nu_{C=O}$ 1691 (m) cm^{-1}. IR (MeCN): $\nu_{C\equiv O}$ 2073 (s), 2035 (vs), 1997 (vs); $\nu_{C=O}$ 1691 (m) cm^{-1}. ^1H NMR (400 MHz, $CDCl_3$): 2.31 (s, 3H, $COCH_3$), 2.74 (s, 2H, NCH_2CH_2S), 2.86 (s, 2H, NCH_2CH_2S), 3.60 (s, 4H, 2NCH_2S) ppm.

Preparation of [(μ-SCH_2)$_2$$NCH_2CH_2O_2CCH_2C_{10}H_7$-1]$Fe_2(CO)_6$ (4). To a solution of **1** (0.179 g, 0.42 mmol) in CH_2Cl_2 (15 mL) cooled to 0 °C were added 1-$C_{10}H_7CH_2C(O)Cl$ (0.14 mL, 0.84 mmol) and pyridine (0.07 mL, 0.84 mmol). The mixture was stirred at 0 °C for 1.5 h and then at room temperature for 16 h. The same workup as that for the preparation of **1** afforded **4** as a red oil (0.191 g, 77%). Anal. Calcd for $C_{22}H_{17}Fe_2NO_8S_2$: C, 44.10; H, 2.86; N, 2.34. Found: C, 43.95; H, 2.68; N, 2.14. IR (KBr disk): $\nu_{C\equiv O}$ 2070 (s), 2024 (vs), 1961 (vs); $\nu_{C=O}$ 1728 (s) cm^{-1}. ^1H NMR (300 MHz, $CDCl_3$): 2.74 (s, 2H, NCH_2CH_2O) , 3.06 (s, 4H, 2NCH_2S), 3.88 (s, 2H, NCH_2CH_2O), 4.02 (s, 2H, $CH_2C_{10}H_7$), 7.35−7.90 (m, 7H, $C_{10}H_7$) ppm.

Preparation of [(μ-SCH_2)$_2$$NCH_2CH_2O_2CCH_2C_{10}H_7$-1]$Fe_2(CO)_5(PPh_3)$ (5). To a red solution of **4** (0.160 g, 0.27 mmol) in MeCN (10 mL) was added $Me_3NO{\cdot}2H_2O$ (0.030 g, 0.27 mmol), and then the mixture was stirred at room temperature for 10 min to give a brown-black solution. After PPh_3 (0.070 g, 0.27 mmol) was added, the new mixture was stirred for 4 h. The same workup as that for the preparation of **1** produced **5** as a red solid (0.185 g, 83%), mp 60−62 °C. Anal. Calcd for $C_{39}H_{32}Fe_2NO_7PS_2$: C, 56.20; H, 3.87; N, 1.68. Found: C, 56.39; H, 4.02; N, 1.87. IR (KBr disk): $\nu_{C\equiv O}$ 2042 (vs), 1981 (vs), 1930 (s); $\nu_{C=O}$ 1734 (s) cm^{-1}. ^1H NMR (300 MHz, $CDCl_3$): 2.18 (s, 2H, NCH_2CH_2O), 2.27, 2.65 (2d, 4H, 2NCH_2S), 3.67 (t, 2H, NCH_2CH_2O), 3.98 (s, 2H, $CH_2C_{10}H_7$), 7.39−7.90 (m, 22H, $C_{10}H_7$, $3C_6H_5$) ppm. ^{31}P NMR (121 MHz, $CDCl_3$, 85% H_3PO_4): 66.02 (s) ppm.

Preparation of [(μ-SCH_2)$_2$$NCH_2CH_2O_2CC_4H_3O$-2]$Fe_2(CO)_6$ (6). A solution of **1** (0.232 g, 0.54 mmol), 2-$C_4H_3OC(O)Cl$ (0.40 mL, 4.06 mmol), and Et_3N (0.80 mL, 5.7 mmol) in CH_2Cl_2 (10 mL) was stirred at room temperature for 5 h to give a brown-red mixture. The same workup as that for the preparation of **1** gave **6** as a red solid (0.224 g, 79%), mp 76−78 °C. Anal. Calcd for $C_{15}H_{11}Fe_2NO_9S_2$: C, 34.31; H, 2.11; N, 2.67. Found: C, 34.45; H, 2.26; N, 2.78. IR (KBr disk): $\nu_{C\equiv O}$ 2074 (s), 2031 (vs), 1994 (vs), 1973 (s); $\nu_{C=O}$ 1728 (s) cm^{-1}. ^1H NMR (400 MHz, $CDCl_3$): 3.10 (s, 2H, NCH_2CH_2O), 3.67 (s, 4H, 2 NCH_2S), 4.17 (s, 2H, NCH_2CH_2O), 6.52, 7.15, 7.59 (3s, 3H, C_4H_3O) ppm.

Preparation of [(μ-SCH_2)$_2$$NCH_2CH_2O_2CC_4H_3S$-2]$Fe_2(CO)_6$ (7). The same procedure was followed as that for the preparation of **6**, but 2-$C_4H_3SC(O)Cl$ (0.55 mL, 5.16 mmol) was used in place of 2-$C_4H_3OC(O)Cl$. **7** was obtained as a red solid (0.178 g, 62%), mp 92−94 °C. Anal. Calcd for $C_{15}H_{11}Fe_2NO_8S_3$: C, 33.29; H, 2.05; N, 2.59. Found: C, 33.42; H, 2.18; N, 2.49. IR (KBr disk): $\nu_{C\equiv O}$ 2070 (s), 2028 (vs), 1985 (vs); $\nu_{C=O}$ 1698 (s) cm^{-1}. IR ($CHCl_3$): $\nu_{C\equiv O}$ 2074 (s), 2036 (vs), 2006 (vs); $\nu_{C=O}$ 1709 (s) cm^{-1}. IR (MeCN): $\nu_{C\equiv O}$ 2073 (s), 2036 (vs), 2000 (vs); $\nu_{C=O}$ 1712 (m) cm^{-1}. ^1H NMR (400 MHz, $CDCl_3$): 3.10 (s, 2H, NCH_2CH_2O) , 3.66 (s, 4H, 2 NCH_2S), 4.16 (s, 2H, NCH_2CH_2O), 7.11, 7.57, 7.77 (3H, C_4H_3S) ppm.

Preparation of [(μ-SCH_2)$_2$$NCH_2CH_2O_2CMe$]$Fe_2(CO)_6$ (8). A mixture of DCC (0.110 g, 0.53 mmol), DMAP (0.034 g, 0.28 mmol), and $CH_2(CO_2H)_2$ (0.024 g, 0.23 mmol) in CH_2Cl_2 (20 mL) was stirred at 0 °C for 1.5 h. To this mixture was added **1** (0.200 g, 0.46 mmol), and the new mixture was stirred at room temperature for 12 h to give a brown-red mixture. The same workup as that for the preparation of **1** afforded **8** as a red solid (0.071 g, 65%), mp 72−73 °C. Anal. Calcd for $C_{12}H_{11}Fe_2NO_8S_2$: C, 30.47; H, 2.34; N, 2.96. Found: C, 30.35; H, 2.45; N, 3.06. IR (KBr disk): $\nu_{C\equiv O}$ 2067 (s), 2030 (vs), 2001 (vs), 1965 (vs); $\nu_{C=O}$ 1742 (s), cm^{-1}. ^1H NMR (400 MHz, $CDCl_3$): 2.02 (s, 3H, CH_3), 2.97 (s, 2H, NCH_2CH_2O), 3.59 (s, 4H, 2NCH_2S), 3.94 (s, 2H, NCH_2CH_2O) ppm. From the second red band **1** (0.093 g) was recovered. When 0.100 g (0.23 mmol) of **1** was used instead of 0.200 g (0.46 mmol) of **1** in the above preparation, 0.073 g (67%) of **8** was obtained.

Preparation of [(μ-SCH_2)$_2$$NCH_2CH_2Fe_2(CO)_6$]$_2$[1,4-$(O_2C)_2C_6H_4$] (9). A mixture of DCC (0.055 g, 0.27 mmol), DMAP (0.017 g, 0.14 mmol), and *p*-$(HO_2C)_2C_6H_4$ (0.019 g, 0.12 mmol) in CH_2Cl_2 (20 mL) was stirred at 0 °C for 1.5 h. To this mixture **1** (0.100 g, 0.23 mmol) was added. The new mixture was stirred at room temperature for 16 h. The same workup as that for the preparation of **1** produced **9** as a red solid (0.050 g, 44%), mp 139 °C (dec). Anal. Calcd for $C_{28}H_{20}Fe_4N_2O_{16}S_4$: C, 33.90; H, 2.03; N, 2.82. Found: C, 34.09; H, 1.92; N, 2.72. IR (KBr disk): $\nu_{C\equiv O}$ 2068 (s), 2031 (vs), 2010 (vs), 1985 (s); $\nu_{C=O}$ 1711 (s) cm^{-1}. ^1H NMR (300 MHz, $CDCl_3$): 3.12 (s, 4H, 2NCH_2CH_2O) , 3.66 (s, 8H, 4NCH_2S), 4.20 (s, 4H, 2NCH_2CH_2O), 8.02 (s, 4H, C_6H_4) ppm.

Protonation Reactions of 3 and 7 with CF_3SO_3H, CF_3CO_2H, or HOAc. (i) ^1H NMR Determination: About 5 mg of **3** or **7** was dissolved in 0.5 mL of $CDCl_3$ in an NMR tube. To this solution was added ca. 10 equiv of CF_3CO_2H (8 μL) or HOAc (6 μL). After the mixture was shaken for 1−2 min, the ^1H NMR spectrum of the resulting new solution was determined. For **3** with CF_3CO_2H, ^1H NMR (400 MHz, $CDCl_3$): 2.44 (s, 3H, $COCH_3$), 3.03 (s, 2H, NCH_2CH_2S), 3.28 (s, 2H, NCH_2CH_2S), 3.78 (s, 4H, 2NCH_2S) ppm. For **3** with HOAc, ^1H NMR (400 MHz, $CDCl_3$): 2.30 (s, 3H, $COCH_3$), 2.74 (s, 2H, NCH_2CH_2S), 2.86 (s, 2H, NCH_2CH_2S), 3.59 (s, 4H, 2NCH_2S) ppm. For **7** with CF_3CO_2H, ^1H NMR (400 MHz, $CDCl_3$): 3.58 (s, 2H, NCH_2CH_2O), 3.82 (s, 4H, 2NCH_2S), 4.49 (s, 2H, NCH_2CH_2O), 7.19, 7.74, 7.89 (3s, 3H, C_4H_3S) ppm. For **7** with HOAc, ^1H NMR (400 MHz, $CDCl_3$): 3.10 (s, 2H, NCH_2CH_2O), 3.67 (s, 4H, 2NCH_2S), 4.16 (s, 2H, NCH_2CH_2O), 7.10, 7.57, 7.77 (3s, 3H, C_4H_3S) ppm.

(ii) IR Determination: About 5 mg of **3** or **7** was dissolved in 0.5 mL of $CHCl_3$ in a test tube. To this solution was added ca. 20 equiv of CF_3CO_2H (15 μL). After it was shaken for 1−2 min, the IR spectrum of the resulting new solution was determined. For **3** with CF_3CO_2H, IR ($CHCl_3$): $\nu_{C\equiv O}$ 2092 (s), 2074 (s), 2055 (vs), 2035 (vs), 2001(vs) cm^{-1}. For **7** with CF_3CO_2H, IR ($CHCl_3$): $\nu_{C\equiv O}$ 2091 (m), 2074 (vs), 2054 (s), 2036 (vs), 2004 (vs) cm^{-1}. About 5 mg of **3** or **7** was dissolved in 0.5 mL of MeCN in a test tube. To this solution was added ca. 1 equiv of CF_3SO_3H (1 μL). After the mixture was shaken for 1−2 min, the IR spectrum of the resulting new solution was determined. For **3** with CF_3SO_3H, IR (MeCN): $\nu_{C\equiv O}$ 2090 (s), 2053 (vs), 2018 (vs) cm^{-1}. For **7** with CF_3SO_3H, IR (MeCN): $\nu_{C\equiv O}$ 2090 (s), 2053 (vs), 2019 (vs) cm^{-1}.

Table 3. Crystal Data and Structure Refinement Details for 3, 7, and 8

	3	**7**	**8**
mol formula	$C_{12}H_{11}Fe_2NO_7S_3$	$C_{15}H_{11}Fe_2NO_8S_3$	$C_{12}H_{11}Fe_2NO_8S_2$
mol wt	489.10	541.13	473.04
cryst syst	monoclinic	monoclinic	triclinic
space group	*C*2/c	*C*2/c	$P\bar{1}$
a/Å	20.431(2)	36.383(9)	7.5467(12)
b/Å	14.3819(17)	8.623(2)	1.5639(2)
c/Å	12.9839(15)	14.270(3)	11.6480(13)
α/deg	90	90	116.801(8)
β/deg	99.376(2)	110.591(4)	90.823(7)
γ/*deg*	90	90	102.403(8)
V/Å^3	3764.2(8)	4191.2(17)	878.9(2)
Z	8	8	2
D_c/g cm^{-3}	1.726	1.715	1.787
abs coeff/mm^{-1}	1.906	1.725	1.927
F(000)	1968	2176	476
index ranges	$-14 \le h \le 25$	$-43 \le h \le 31$	$-9 \le h \le 9$
	$-17 \le k \le 16$	$-10 \le k \le 10$	$-15 \le k \le 15$
	$-15 \le l \le 16$	$-8 \le l \le 16$	$-15 \le l \le 15$
no. of rflns	10 444	10 349	10 870
no.of indep rflns	3798	3689	4157
$2\theta_{max}$/deg	52.68	50.04	55.74
R	0.0309	0.0363	0.0267
R_w	0.0595	0.0995	0.0551
goodness of fit	1.021	1.049	0.977
largest diff peak and hole/e Å^{-3}	0.267/−0.251	0.621/−0.532	0.410/−0.457

X-ray Structure Determinations of 1, 3, 7, and 8. Single crystals of **1**, **3**, **7**, and **8** suitable for X-ray diffraction analyses were grown by slow evaporation of the CH_2Cl_2/hexane solutions of **1**, **7**, and **8** at −10 °C or the CH_2Cl_2/petroleum ether solution of **3** at −20 °C, respectively. A single crystal of **1**, **3**, **7**, or **8** was mounted on a Bruker SMART 1000 automated diffractometer. Data were collected at room temperature by using a graphite monochromator with Mo Kα radiation ($\lambda = 0.71073$ Å) in the $\omega-\phi$ scanning mode. Absorption correction was performed by the SADABS program.[41] The structures were solved by direct methods using the SHELXS-97 program[42] and refined by full-matrix least-squares techniques (SHELXL-97)[43] on F^2. Hydrogen atoms were located using the geometric method. Details of crystal data, data collections, and structure refinements are summarized in Table 3.

Electrochemistry. Acetonitrile (Fisher Chemicals, HPLC grade) was used in electrochemical experiments. A solution of 0.1 M *n*-Bu_4NPF_6 in MeCN was used as electrolyte in all cyclic voltammetric experiments. Electrochemical measurements were made using a BAS Epsilon potentiostat. All voltammograms were obtained in a three-electrode cell with a 3 mm diameter glassy carbon working electrode, a platinum counter electrode, and an Ag/Ag^+ (0.01 M $AgNO_3$/0.1 M *n*-Bu_4NPF_6 in MeCN) reference electrode under CO atmosphere. The working electrode was polished with 0.05 μm alumina paste and sonicated in water for 10 min prior to use. Bulk electrolysis was run on a vitreous carbon rod (ca. 3 cm^2) in a two-compartment, gastight, H-type electrolysis cell containing ca. 20 mL of MeCN. All potentials are quoted against the ferrocene/ferrocenium (Fc/Fc^+) potential. Gas chromatography was performed with a Shimadzu GC-9A gas chromatograph under isothermal conditions with nitrogen as a carrier gas and a thermal conductivity detector.

Acknowledgment. We are grateful to the National Natural Science Foundation of China and the Research Fund for the Doctoral Program of Higher Education of China for financial support.

Supporting Information Available: Full tables of crystal data, atomic coordinates and thermal parameters, and bond lengths and angles for **1**, **3**, **7**, and **8** as CIF files. This material is available free of charge via the Internet at http://pubs.acs.org.

OM7005326

(41) Sheldrick, G. M. *SADABS, A Program for Empirical Absorption Correction of Area Detector Data*; University of Göttingen: Germany, 1996.

(42) Sheldrick, G. M. *SHELXS97, A Program for Crystal Structure Solution*; University of Göttingen: Germany, 1997.

(43) Sheldrick, G. M. *SHELXL97, A Program for Crystal Structure Refinement*; University of Göttingen: Germany, 1997.